Integral Representation in the Hodograph Plane for Compressible Flow Problems

Erik B. Hansen
Department of Mathematics
Technical University of Denmark
DK 2800 Lyngby, Denmark

George C. Hsiao
Department of Mathematical Sciences
University of Delaware
Newark, DE 19716

Technical Report No. 2000–9

Integral Representation in the Hodograph Plane for Compressible Flow Problems

Erik B. Hansen[1] and George C. Hsiao[2]

December 7, 1999

[1]Department of Mathematics, Technical University of Denmark, DK 2800, Lyngby, Denmark.

[2]Department of Mathematical Sciences, University of Delaware, Newark, Delaware 19716, USA.

Abstract

Compressible flow is considered in the hodograph plane. The fact that the equation for the stream function is linear there is exploited to derive a representation formula for the stream function, involving boundary data only, and a fundamental solution to the equation. For subsonic flow, an efficient algorithm for computation of the fundamental solution is also developed.

1991 AMS Classification: 35C15, 76G25, 76M15.

1. Introduction

Integral equation methods have been used extensively in fluid mechanics as is evident from a comprehensive review of the field from 1983 by Morino [1] and a more recent one by Pozrikidis [2]. By far the majority of the applications have been to inviscid, incompressible potential flow or to Stokes' flow, where the governing equations (but not necessarily the boundary conditions) are linear, thereby allowing one of the main advantages of integral equation methods, the reduction of the dimension of the problem by one, to be achieved. But integral equation methods have also often been applied to compressible, including transsonic, flow problems, although the equations for compressible flow in the physical plane are non-linear. The pioneer in this field was Ostwatitsch [3]. Many early applications to compressible flows were presented in [4] and [5], and some more recent ones are reviewed in [1]. They are all based directly on the equations in the physical plane, and since the non-linear terms give rise to domain integrals in the representation formula, no reduction of dimension is achieved until further, simplifying approximations, besides the fundamental ones of irrotational and homentropic flow, have been introduced.

Most of the work referred to above deals with two-dimensional problems, and it is well known that in two dimensions the equations for compressible flow become linear when transformed to the hodograph plane. Because of this property the hodograph transformation has often been applied to compressible flow problems. An early application of the hodograph transformation was made by Lighthill in three papers [6], [7], and [8], in which he studied the flow in a symmetric channel as well as the one around a cylindrical body and derived several results on the mathematical properties of the transformation. Other examples of applications to concrete problems are found in [4] and [5], and in [9] the hodograph transformation is used in a theoretical investigation. However, surprisingly enough, despite the fact that an integral equation formulation of a compressible flow problem in the hodograph plane would lead to a *boundary* integral equation and, consequently, to a reduction of dimension by one, this avenue of attack does not seem so far to have been investigated in the litterature.

The purpose of the present paper is to develop tools which are necessary for solving compressible flow problems via boundary integral methods in the hodograph plane. The focus is on subsonic problems. As we shall see, since the fluid velocity at a rigid body surface in the flow region is not known *a priori*, a boundary value problem with fixed boundaries in the physical plane becomes a free boundary problem in the hodograph plane. However, integral equation methods are also well suited for solving free boundary problems and have often been used for that purpose, so this is not a serious drawback.

The rest of this paper is organized as follow. In Section 2 we review, for later reference, the equations for compressible flow in the physical as well as in the hodograph plane, and we formulate a typical, subsonic boundary value problem in the hodograph plane. In Section 3 we set up one of the two main tools of integral equation formulations, namely a representation formula for solutions to the partial differential equation in question. The other main tool is a fundamental solution. In Section 4 we construct one, and in Section 5 we describe its numerical evaluation in the subsonic region. The extension to the supersonic region and applications to specific flow problems will be considered later.

2. Boundary value problems in the hodograph plane.

For stationary, two-dimensional, compressible flow of an inviscid fluid the equations of motion are

$$\rho(uu_x + vu_y) + p_x = 0 \quad \text{and} \quad \rho(uv_x + vv_y) + p_y = 0, \tag{1}$$

and the continuity equation is

$$(\rho u)_x + (\rho v)_y = 0. \tag{2}$$

Here ρ is the density, p the pressure, and (u, v) the velocity referred to a rectangular $xy-$coordinate system. We shall treat the fluid as an ideal gas and assume that the flow is irrotational and homentropic. Then,

$$u_y = v_x \tag{3}$$

and the quantity

$$\frac{p}{\rho^\gamma} = \frac{p_0}{\rho_0^\gamma} \tag{4}$$

is a global constant in the fluid region. The quantities p_0 and ρ_0 introduced here shall denote the values of p and ρ, respectively, at a stagnation point (it follows from (6) and (8), below, that p and ρ assume the same values at all stagnation points). The constant γ in (4) is Poisson's ratio between the specific heats. For air $\gamma = 1.41$.

For an ideal gas the speed of sound is equal to

$$c = \sqrt{\frac{dp}{d\rho}} = \sqrt{\gamma\frac{p}{\rho}}. \tag{5}$$

From (4) and (5) it is seen that p and ρ can be expressed as

$$p = p_0(\frac{c}{c_0})^{\frac{2\gamma}{\gamma-1}} \text{ and } \rho = \rho_0(\frac{c}{c_0})^{\frac{2}{\gamma-1}}, \tag{6}$$

where c_0 is the speed of sound at a stagnation point. It follows from (1), (2), and (5) that

$$(u^2 - c^2)u_x + uv(u_y + v_x) + (v^2 - c^2)v_y = 0. \tag{7}$$

Application of (3) and (6) in (1) leads to *Bernoulli's equation*:

$$c^2 = c_0^2 - \frac{(\gamma - 1)}{2}q^2, \tag{8}$$

in which $q = (u^2 + v^2)^{1/2}$. Since c cannot be negative, equation (8) shows that the mathematical description of a flow based on (1), (2), (3), and (4) implies that q cannot exceed the value

$$q_{max} = \sqrt{\frac{2}{\gamma - 1}} c_0. \tag{9}$$

We also see that $c = q$ at the so-called critical speed,

$$q_{crit} = \sqrt{\frac{2}{\gamma + 1}} c_0. \tag{10}$$

Therefore a flow is called *subsonic* at a point where $q < q_{crit}$, and *supersonic* at a point where $q > q_{crit}$.

If the continuity equation is satisfied in a simply connected region, ρu and ρv can be expressed in terms of a stream function, ψ, as

$$\rho u = \psi_y \quad \text{and} \quad \rho v = -\psi_x. \tag{11}$$

A stream function also exists for flows in multiply connected regions, if the imbedded obstacles have impermeable walls. When ρ is inserted from (6) and the resulting expressions are differentiated with respect to x and y, (3) and (7) can be used to derive the following equation for the stream function:

$$(1-\frac{u^2}{c^2})\frac{\partial^2\psi}{\partial x^2}-\frac{2uv}{c^2}\frac{\partial^2\psi}{\partial x\partial y}+(1-\frac{v^2}{c^2})\frac{\partial^2\psi}{\partial y^2}=0. \tag{12}$$

In order to derive an equation for the stream function in the hodograph plane we introduce a velocity potential, ϕ, defined by the relations $u=\phi_x$ and $v=\phi_y$, which are in accordance with (3). Then

$$u=\phi_x=\phi_u u_x+\phi_v v_x \text{ and } -\rho v=\psi_x=\psi_u u_x+\psi_v v_x. \tag{13}$$

Using these relations and the corresponding ones involving the $y-$derivatives, we first find expressions for u_x, u_y, v_x and v_y in terms of ϕ_u, ϕ_v, ψ_u, and ψ_v. By inserting the expressions into (3) and (7) we thereafter find ϕ_u and ϕ_v expressed in terms of u, v, ψ_u, and ψ_v. Finally, by cross differentiation with respect to u and v, we obtain the equation

$$(1-\frac{v^2}{c^2})\frac{\partial^2\psi}{\partial u^2}+\frac{2uv}{c^2}\frac{\partial^2\psi}{\partial u\partial v}+(1-\frac{u^2}{c^2})\frac{\partial^2\psi}{\partial v^2}+\frac{2}{c^2}(u\frac{\partial\psi}{\partial u}+v\frac{\partial\psi}{\partial v})=0. \tag{14}$$

We also use the expressions for ϕ_u and ϕ_v to derive the following formulas for the derivatives of the fluid speed, q_x and q_y, which we shall need later:

$$q_x = -D\psi_v, \quad \text{and} \quad q_y = D\psi_u, \tag{15}$$

where

$$D = \frac{\rho q c^2}{(c^2 - v^2)\psi_u^2 + 2uv\psi_u\psi_v + (c^2 - u^2)\psi_v^2}. \tag{16}$$

Having obtained equation (14) for the stream function, we now proceed to considering the boundary conditions for ψ in the hodograph plane. Let the curve Γ in Figure 1 be the intersection with the physical plane of a rigid, impermeable cylinder, and let C be its image in the hodograph plane. The definition of the polar coordinates, q and θ, in the hodograph plane is indicated in the figure. At an arbitrary point, P_Γ, on Γ the fluid velocity is parallel to the tangent there. So, the polar, angular coordinate of the image, P_C, of P_Γ is equal to the angle between the tangent of Γ at P_Γ and the x-axis. However, the fluid speed at P_Γ is not known *a priori*, and therefore the radial coordinate, q, of P_C, and hence the location of the entire image of Γ, is unknown. Thus a problem with rigid boundaries in the physical plane becomes a free boundary problem when transformed to the hodograph plane. This fact was pointed out by Nocilla [10], who also derived a boundary condition equivalent to our formula (20), below.

Since the stream function assumes a constant value on a rigid boundary, Γ, in the physical plane, it assumes the same constant value on the image, C, in the hodograph plane. Since the image is a free boundary, we expect more than one condition to be satisfied by ψ on C, and because equation (14) is of second order, we anticipate that there are precisely two such conditions. In order to find the second condition we write the equation for C as $q = f(\theta)$ (assuming that Γ in not a straight line) and consider the derivative of the fluid speed with respect to the arc length, σ, on Γ. It can be expressed as

$$\frac{dq}{d\sigma} = \frac{dq}{d\theta}\frac{d\theta}{d\sigma} = f'(\theta)\kappa(\theta), \tag{17}$$

if the curvature, κ, of Γ is defined as $\kappa(\theta) = d\theta/d\sigma$. The derivative can also be expressed as

$$\frac{dq}{d\sigma} = q_x cos\theta + q_y sin\theta = q_x\frac{u}{q} + q_y\frac{v}{q}. \tag{18}$$

When the expressions for q_x and q_y in (15) are used, (17) and (18) combine to give:

$$f'(\theta)\kappa = \frac{\rho c^2(-u\psi_v + v\psi_u)}{(c^2 - v^2)\psi_u^2 + 2uv\psi_u\psi_v + (c^2 - u^2)\psi_v^2}. \tag{19}$$

If $\mathbf{T} = (T_u, T_v)$ denotes the tangent of C, the fact that ψ is constant on C implies that $\psi_u T_u + \psi_v T_v = 0$, and if the normal to C is defined as indicated in Figure 1, the derivatives can be expressed as $\psi_u = -T_v \partial\psi/\partial N$ and $\psi_v = T_u \partial\psi/\partial N$. When these expressions are inserted in (19), the following formula for the normal derivative is obtained:

$$\frac{\partial\psi}{\partial N} = \frac{-\rho c^2 \mathbf{T}\cdot\mathbf{q}}{[c^2 - (\mathbf{T}\cdot\mathbf{q})^2]\kappa f'(\theta)}. \tag{20}$$

Here $\mathbf{q}=(u, v)$.

We are now in a position to formulate a subsonic, compressible flow problem as a boundary value problem in the hodograph plane. As a simple example we consider the flow around a cylindrical, symmetric airfoil, which is introduced in a uniform flow with speed q_∞ in such a way that its symmetry axis is parallel to the undisturbed flow direction (see Figure 2). On the symmetry axis upstream from the airfoil the velocity is parallel to the $x-$axis and the speed decreases from q_∞ at infinity to 0 at the edge of the airfoil. (The opening angle, $2\theta_1$, is assumed to be larger than 0.) Therefore the image of the upstream part of the symmetry axis is the line section $C_S = \{\theta, q \mid \theta = 0, 0 < q < q_\infty\}$. On the upper side of the airfoil the velocity first points in the direction $\theta = \theta_1$. As the upper half of the coutour is transversed the direction of the velocity turns clock-wise, and its direction at the downstream edge, where $q = 0$ again, is $\theta = -\theta_2$. So, the image of the upper half of the contour is a curve, C_A, indicated in Figure 3, which leaves the origin, $q = 0$, in the direction $\theta = \theta_1$ and returns to the origin from the direction $\theta = -\theta_2$. The image of the top point, P_T, on the airfoil is the intersection of C_A with the $u-$axis. The symmetry line downstream from the airfoil is mapped onto the same line section, C_S as the upstream part. Thus, the image of the flow field in the upper half of the physical plane is the region bounded by C_A and cut along C_S. On C_S and on C_A, ψ assumes one and the same constant value. On C_A, ψ also satisfies condition (20).

3. The representation formula

In order to derive a representation formula for solutions to equation (14) we consider an integral

$$\int_\Omega G L\psi d\Omega = 0. \tag{21}$$

This formula and all other expressions in the following derivation of the representation formula are to be interpreted in the sense of distribution theory. In the integral Ω is a bounded region in the hodograph plane, G is a fundamental solution to an equation to be chosen later, $L\psi$ denotes the left hand side of equation (14), and ψ is a solution to equation (14) everywhere in Ω. Therefore the integral vanishes.

In order to arrive eventually at a form of the integrand in which there are no derivatives of ψ, we write the product of G and the first term of $L\psi$ as follows:

$$G(1-\frac{v^2}{c^2})\frac{\partial^2\psi}{\partial u^2} = \tag{22}$$

$$\frac{\partial}{\partial u}((1-\frac{v^2}{c^2})G\frac{\partial\psi}{\partial u}) - (1-\frac{v^2}{c^2})\frac{\partial G}{\partial u}\frac{\partial\psi}{\partial u} + \frac{uv^2}{c^4}(\gamma-1)G\frac{\partial\psi}{\partial u}.$$

When the other terms are recast in similar ways we find by repeated application of Gauss' formula that (21) can also be written

$$\int_{\partial\Omega} B(G,\psi)ds + \int_{\Omega}\psi\tilde{L}Gd\Omega = 0. \tag{23}$$

Here s is the arclength along the boundary, $\partial\Omega$, of Ω,

$$B(G,\psi) = \left[(1-\frac{v^2}{c^2})(G\frac{\partial\psi}{\partial u} - \psi\frac{\partial G}{\partial u}) + \frac{uv}{c^2}(G\frac{\partial\psi}{\partial v} - \psi\frac{\partial G}{\partial v}) + \frac{u}{c^2}G\psi\right] N_u$$

$$+\left[(1-\frac{u^2}{c^2})(G\frac{\partial\psi}{\partial v} - \psi\frac{\partial G}{\partial v}) + \frac{uv}{c^2}(G\frac{\partial\psi}{\partial u} - \psi\frac{\partial G}{\partial u}) + \frac{v}{c^2}G\psi\right] N_v, \tag{24}$$

and

$$\tilde{L}G = (1 - \frac{v^2}{c^2})\frac{\partial^2 G}{\partial u^2} + \frac{2uv}{c^2}\frac{\partial^2 G}{\partial u \partial v} + (1 - \frac{u^2}{c^2})\frac{\partial^2 G}{\partial v^2} - \frac{2c_0}{c^4}G. \qquad (25)$$

We now choose G to be a fundamental solution to the equation $\tilde{L}w = 0$, that is $G = G(u, v, u', v')$, and

$$\tilde{L}G = -\delta(u - u')\delta(v - v'), \qquad (26)$$

where δ is Dirac's delta function. It then follows from (23) that if (u', v') is a point in the interior of Ω, $\psi(u', v')$ can be expressed as

$$\psi(u', v') = \int_{\partial\Omega} B(G, \psi)ds. \qquad (27)$$

It is also seen that if (u', v') is neither in the interior of Ω nor on $\partial\Omega$, the integral in (27) vanishes. Formula (27) is a representation formula for solutions to the equation for the stream function in the hodograph plane.

Since the boundary conditions in the hodograph plane are conveniently expressed in terms of the normal and tangential derivatives of ψ, we choose to write the integrand $B(\psi, G)$ given by (24) in terms of the same derivatives. If the unit tangent and normal vectors, $\mathbf{T}$ and $\mathbf{N}$, are oriented as shown in

Figure 1, $(T_u, T_v) = (N_v, -N_u)$. If these relations and the formulas

$$\frac{\partial f}{\partial u} = \frac{\partial f}{\partial s} T_u + \frac{\partial f}{\partial N} N_u \quad \text{and} \quad \frac{\partial f}{\partial v} = \frac{\partial f}{\partial s} T_v + \frac{\partial f}{\partial N} N_v \tag{28}$$

for the derivatives of a function f of u and v are used in (27), the representation formula becomes

$$\psi(u', v') = \tag{29}$$

$$\int_{\partial\Omega} \left[(1 - \frac{(\mathbf{q} \cdot \mathbf{T})^2}{c^2})(G \frac{\partial \psi}{\partial N} - \psi \frac{\partial G}{\partial N}) + \frac{\mathbf{q} \cdot \mathbf{T}\, \mathbf{q} \cdot \mathbf{N}}{c^2} (G \frac{\partial \psi}{\partial s} - \psi \frac{\partial G}{\partial s}) + \frac{\mathbf{q} \cdot \mathbf{N}}{c^2} G \psi \right] ds.$$

Based on this formula and boundary conditions, such as those presented in section 2, an integral equation formulation, similar to those used in [11] and [12] to other free boundary problems, can be derived.

4. A fundamental solution

As the fundamental solution, G, entering in the representation formula we choose the one which is bounded at $q = 0$ and vanishes at $q = q_{max}$.

With the polar hodograph coordinates, q and θ, used as independent variables equation (26) reads:

$$\frac{\partial^2 G}{\partial q^2} + \frac{1-M^2}{q}\frac{\partial G}{\partial q} + \frac{1-M^2}{q^2}\frac{\partial^2 G}{\partial \theta^2} - \frac{2c_0^2}{c^4}G = -\frac{\delta(q-q')\delta(\theta-\theta')}{q}, \qquad (30)$$

where $M = q/c$. Since this equation and the boundary conditions for G are symmetric with respect to the ray $\theta = \theta'$, the Fourier series of G has the form

$$G(q,q',\theta-\theta') = \sum_{n=0}^{\infty} G_n cos(n(\theta-\theta')) = \sum_{n=0}^{\infty} A_n Q_n(q) cos(n(\theta-\theta')). \qquad (31)$$

Here A_n is a coefficient depending on q' and Q_n is a solution to the equation

$$\frac{d^2 Q_n}{dq^2} + \frac{1-M^2}{q}\frac{dQ_n}{dq} - (\frac{2c_0^2}{c^4} + \frac{1-M^2}{q^2}n^2)Q_n = -\frac{\delta(q-q')}{\pi q(1+\delta_{0n})}, \qquad (32)$$

where δ_{0n} is Kronecker's delta.

By the transformation

$$w = 1 - \frac{c^2}{c_0^2} = \frac{\gamma-1}{2}\frac{q^2}{c_0^2} \qquad (33)$$

equation (32) becomes:

$$\frac{d^2Q_n}{dw^2}+\left[\frac{1}{w}-\frac{1}{(\gamma-1)(1-w)}\right]\frac{dQ_n}{dw}- \tag{34}$$

$$\left[\frac{1}{(\gamma-1)(1-w)}+\frac{n^2}{4w}-\frac{n^2(\gamma+1)}{4(\gamma-1)}\right]\frac{Q_n}{w(1-w)}=-\frac{\delta(w-w')}{2\pi(1+\delta_{0n})w},$$

where w' is the value of w for $q=q'$.

The homogeneus equation corresponding to (34) has regular singularities at $w=0$ and $w=1$. The exponents of the solutions are $n/2$ and $-n/2$ at $w=0$ and 1 and $-1/(\gamma-1)$ at $w=1$. The point at infinity turns out to be a regular singularity, too. Thus, the equation has precisely three singular points, which are all regular singularities, and therefore its solutions can be expressed in terms of hypergeometric functions. Indeed, when its solutions are written as

$$Q_n(q)=w^{-n/2}(1-w)^{-1/(\gamma-1)}P_n(w), \tag{35}$$

the equation for P_n becomes the hypergeometric equation,

$$w(1-w)\frac{d^2P_n}{dw^2}+\left[1-n-(1-n-\frac{1}{\gamma-1})w\right]\frac{dP_n}{dw}+\frac{n(n-1)}{2(\gamma-1)}P_n=0. \tag{36}$$

In the following we shall consider two solutions to (36). For the one, denoted by R_n, the corresponding function Q_n is bounded at $w = 0$. For the other one, S_n, the corresponding function Q_n vanishes at $w = 1$. Using standard separation of variables technique we then find the series in (31) to be

$$G(q, q', \theta - \theta') = -\frac{1}{2\pi(1-w)^{1/(\gamma-1)}} \sum_{n=0}^{\infty} \frac{R_n(w_<)S_n(w_>)}{(ww')^{n/2}(1+\delta_{0n})C_n} cos(n(\theta - \theta')), \tag{37}$$

where $w_<$ is the smaller and $w_>$ the larger of w and w', and the constant C_n is determined from the Wronskian:

$$R_n \frac{dS_n}{dw} - S_n \frac{dR_n}{dw} = C_n w^{n-1}(1-w)^{1/(\gamma-1)}. \tag{38}$$

For $n = 0$ equation (36) has constant solutions. A solution linearly independent of a constant is found by quadrature, and the resulting integral can be expanded in a power series and integrated termwise. In this way we get two solutions of the types defined above, namely:

$$R_0(w) = 1 \quad \text{and} \quad S_0(w) = -(1-w)^{1/((\gamma-1)} \left[ln(w) + \sum_{k=1}^{\infty} \frac{(1-w)^k}{k((\gamma-1)k+1)} \right]. \tag{39}$$

For $n = 1$, too, the equation has constants solutions and the function

$S_1 = (1-w)^{\gamma/(\gamma-1)}$ is another closed form solution. Therefore, for $n = 1$ we define:

$$R_1(w) = 1 - (1-w)^{\gamma/(\gamma-1)} \quad \text{and} \quad S_1(w) = (1-w)^{\gamma/(\gamma-1)}. \tag{40}$$

For $n > 1$ the solutions can be expressed by means of hypergeometric functions defined by the usual formula:

$$F(a,b;c;z) = \frac{\Gamma(c)}{\Gamma(a)\Gamma(b)} \sum_{k=0}^{\infty} \frac{\Gamma(a+k)\Gamma(b+k)}{\Gamma(c+k)k!} z^k \tag{41}$$

(see *e.g.* [13]). We define the following two solutions:

$$R_n(w) = w^n F(\alpha+n, \beta+n; n+1; w) \tag{42}$$

and

$$S_n(w) = \frac{\Gamma(1-\alpha)\Gamma(1-\beta)}{(n-1)!\Gamma(\frac{2\gamma-1}{\gamma-1})}(1-w)^{\gamma/(\gamma-1)} F(\alpha+\frac{\gamma}{\gamma-1}, \beta+\frac{\gamma}{\gamma-1}; \frac{2\gamma-1}{\gamma-1}; 1-w). \tag{43}$$

Here α and β are the two constants:

$$\left.\begin{matrix}\alpha\\ \\ \beta\end{matrix}\right\} = -\frac{n}{2} - \frac{1}{2(\gamma-1)} \pm \frac{(n^2(\gamma^2-1)+1)^{1/2}}{2(\gamma-1)}. \tag{44}$$

In S_n, the constant coefficient is chosen so that $S_n(0) = 1$ (see formula (46), below).

The series for R_n converges slowly as the singularity at $w = 1$ is approached, and the same holds with regard to S_n as w approches 0. In order to be able to compute the functions numerically for all $\in [0, 1]$ and to find the constants C_n from (38) we construct alternative expressions for the two functions from formulas found in [13]. For R_n, application of formulas (15.3.3) and (15.3.6) in [13] results in the expression:

$$R_n(w) = \frac{n!\Gamma(\frac{\gamma}{\gamma-1})}{\Gamma(1-\alpha)\Gamma(1-\beta)} F(\alpha, \beta; -\frac{1}{\gamma-1}; 1-w) + \tag{45}$$

$$(1-w)^{\gamma/(\gamma-1)} \frac{n!\Gamma(-\frac{\gamma}{\gamma-1})}{\Gamma(\alpha+n)\Gamma(\beta+n)} F(\alpha + \frac{\gamma}{\gamma-1}, \beta + \frac{\gamma}{\gamma-1}; \frac{2\gamma-1}{\gamma-1}; 1-w),$$

in which the series in (41) can be used. For S_n a series, which converges repidly near $w = 0$, is found from (15.3.11) in [13]:

$$S_n(w) = \tag{46}$$

$$(1-w)^{\gamma/(\gamma-1)} \left\{ \sum_{k=0}^{n-1} \frac{\Gamma(1-\alpha-n+k)\Gamma(1-\beta-n+k)(n-1-k)!}{\Gamma(1-\alpha-n)\Gamma(1-\beta-n)k!(n-1)!}(-w)^k - \right.$$

$$\left. \frac{(-w)^n}{(n-1)!} \sum_{k=0}^{\infty} \frac{\Gamma(1-\alpha+k)\Gamma(1-\beta+k)}{\Gamma(1-\alpha-n)\Gamma(1-\beta-n)k!(k+n)!} w^k [log(w) - p_{n,k}] \right\}.$$

Here

$$p_{n,k} = \psi(k+1) + \psi(k+n+1) - \psi(1-\alpha+k) - \psi(1-\beta+k), \tag{47}$$

where ψ has the usual meaning, $\psi(z) = \Gamma'(z)/\Gamma(z)$.

Using (42) for R_n and (46) for S_n at $w = 0$ (or (45) for R_n and (43) for S_n at $w = 1$) we find the constants C_n in (37) and (38) to be:

$$C_0 = -1, \quad C_1 = -\frac{\gamma}{\gamma-1} \text{ and } C_n = -n \text{ for } n > 1. \tag{48}$$

The final formula for G is now obtained, when the various expressions derived above are inserted in (37).

5. Numerical evaluation of the fundamental solution

Although we now have at our disposal two series expansions for each function, R_n and S_n, of which the one converges rapidly near $w = 0$, and the other one near $w = 1$, they are not sufficient for accurate, double precision computation for all values of w. The reason is that for values of w in the central part of the interval $[0, 1]$, the ratio between the sum of any of the infinite series', we are considering, and its largest term decreases with increasing n, and for n sufficiently large, the ratio is too small for double precision accuracy (10^{-16}). In order to be able to compute R_n and S_n for all w we therefore also use series expansions with expansion points in the interior of the interval $[0, 1]$. It is found that if $w_0 \in]0, 1[$, the coefficients of a series:

$$P_n(w) = \sum_{k=0}^{\infty} b_k (w - w_0)^k. \tag{49}$$

for a solution to equation (36) are determined by the following three term recursion formula:

$$b_{k+2} = \frac{(2w_0-1)k - \frac{w_0}{\gamma-1} + (n-1)(1-w_0)}{(k+2)w_0(1-w_0)} b_{k+1} + \tag{50}$$

$$\frac{k(k-n-\frac{1}{\gamma-1}) - \frac{1}{2}n(n-1)\frac{1}{\gamma-1}}{(k+1)(k+2)w_0(1-w_0)} b_k.$$

In our computations we apply the system of series' in the following way: We first use (42), (43), (45), and (46) to compute $R_n(w_0)$ and $S_n(w_0)$ and the first derivatives, $R_n'(w_0)$ and $S_n'(w_0)$ with quadrouple precision accuracy (32 digits), at $w_0 = 1/3$ and $w_0 = 2/3$. The results are thereafter inserted for b_0 and b_1 in (50) and the required number of the coefficients b_k in (49) are found using double precision calculation. In this way we are able to evaluate $R_n(w)$ and $S_n(w)$ with double precision accuracy for n up to 50 and all $w \in [0,1]$ by means of the pair of series' of which the expansion point, $w_0 = 0,\ 1/3,\ 2/3$, or 1, is closest to w.

In the elliptic region (subsonic flow), fundamental solutions diverge towards infinity as the field point, (q,θ), approaches the singular point, (q',θ'). Therefore the rate of convergence of the series in (37) is poor for field points near the singular point. In order to be able to compute G there also, we need a closed form expression with the same singular behavior near (q',θ') as that of a fundamental solution. If G^* donotes such an expression, and G_n^* its n'th

Fourier coefficient, the series in the formula

$$G = G^* + \sum_{n=0}^{\infty}(G_n - G_n^*)cos(n(\theta - \theta')) \qquad (51)$$

converges more rapidly than the one in (37), if (q, θ) is close to (q', θ').

In order to construct a function, G^*, we rely upon the intuitive assumption that the leading term of a fundamental solution at the singular point is not changed if the coefficients in equation (30) are 'frozen' at the singular point, *i.e.* the coefficients are replaced by constants equal to their respective values at that point. With the new independent variables ξ and η defined by

$$\xi = qcos(\theta - \theta') - q' \;\; \text{and} \;\; \eta = qsin(\theta - \theta') \qquad (52)$$

equation (30) reads

$$(1 - \frac{\eta^2}{c^2})\frac{\partial^2 G}{\partial \xi^2} + 2\frac{\xi\eta}{c^2}\frac{\partial^2 G}{\partial\xi\partial\eta} + (1 - \frac{(\xi + q')^2}{c^2})\frac{\partial^2 G}{\partial\eta^2} - 2\frac{c_0^2}{c^4}G = -\delta(\xi)\delta(\eta). \quad (53)$$

Here we freeze the coefficients by putting $\xi = \eta = 0$ and $c = c' \equiv c(q')$ and introduce the new variable $t = \eta(1 - q'^2/c'^2)^{-1/2}$. The resulting equation,

$$\frac{\partial^2 G^*}{\partial \xi^2} + \frac{\partial^2 G^*}{\partial t^2} - 2\frac{c_0^2}{c'^4}G^* = -(1 - q'^2/c'^2)^{-1/2}\delta(\xi)\delta(t), \tag{54}$$

has the solution

$$\frac{1}{2\pi\sqrt{1 - q'^2/c'^2}}K_0(\frac{\sqrt{2}c_0}{c'^2}\sqrt{\xi^2 + t^2}), \tag{55}$$

where K_0 is the modified Bessel function of the third kind, order 0. This function could be used for G^*, but since its Fourier coefficients cannot be expressed in closed form, but must be evaluated by numerical quadrature, it is difficult to compute them accurately, if q is close to q'. Therefore we use the leading term of (55), only, for G^*. Expressed in terms of the original variables, q and θ, the leading term is

$$G^* = -\frac{1}{4\pi\sqrt{1 - q'^2/c'^2}} ln((q cos(\theta - \theta') - q')^2 + \frac{q^2 sin^2(\theta - \theta')}{1 - q'^2/c'^2}). \tag{56}$$

Using formulas given in [14] we find the Fourier coefficients of G^* to be:

$$G_0^* = ln\left[\frac{(a_1 + \sqrt{a_1^2 - b^2})(a_2 + \sqrt{a_2^2 - b^2})}{4(c'^2 - q'^2)}\right] \tag{57}$$

and

$$G_n^* = -\frac{2}{n}\sum_{k=1}^{k=2}\left[\frac{\sqrt{a_k^2-b^2}-a_k}{b}\right]^n \tag{58}$$

for $n > 0$, where

$$a_k = c'\sqrt{c'^2+q^2-q'^2}+(-1)^k(c'^2-q'^2), \tag{59}$$

and $b = qq'$.

The fundamental solution G is now easily computed everywhere in the subsonic region. Graphs of G for various values of (q', θ') with $\theta' = 0$ are presented in Figures 4 through 9.

References.

[1] Morino, L., Boundary integral equations in aerodynamics, Appl. Mech. Rev., **46**, no 8, 445-466, 1983.

[2] Pozrikidis, C., Boundary Integral and Singular Methods for Linearized Viscous Flow, Cambridge University Press, Cambridge, 1992.

[3] Oswatitsch, K., Die Geschwindigkeitverteilung bei lokalen Überschallgebiete an flachen Profilen, Z. angew. Math. Mech., **30**, 17-24, 1950.

[4] Symposium Transsonicum, K. Oswatitsch, Ed., Springer, Berlin, 1964.

[5] Symposium Transsonicum II, K. Oswatitsch and D. Rues, Eds., Springer, Berlin, 1976.

[6] Lighthill, M. J., The hodograph transformation in trans-sonic flow. I. Symmetric channels, Proc. Roy. Soc. London, Ser.A **191**, 323-341.

[7] Lighthill, M. J., The hodograph transformation in trans-sonic flow. II. Auxiliary theorems on the hypergeometric functions $\psi_n(\tau)$, Proc. Roy. Soc. London, Ser.A **191**, 341-351.

[8] Lighthill, M. J., The hodograph transformation in trans-sonic flow. III. Flow round a body,, Proc. Roy. Soc. London, Ser.A **191**, 352-369.

[9] Shimborsky E., Variational methods applied to the study of symmetric flows in Laval nozzles, Comm. Partial Differential Equations, **4**, 41-77,1979.

[10] Nocilla S., Sull'esistenza di flussi transonici continui attorne a profili alari ad arco cerchio, Atti della Academia delle Scienzi di Torino, **94**, 796-822, 1960.

[11] Hansen, Erik B., Stokes flow down a wall into an infinite pool. J. Fluid Mech. **178**, 243-256.

[12] Hansen, Erik B. and Kelmanson, Mark A., Steady, viscous, free-surface flow on a rotating cylinder. J. Fluid Mech. **272**, 291-107.

[13] Abramowitz, M. and Stegun, I., Handbook of Mathematical Functions, Dover Publications, New York, 9th. printing, 1970, p.562-564.

[14] Gröbner, W. and Hofreiter, N., Integraltafel, Zweiter Teil, Bestimmte Integrale. Springer, Wien, 5th. ed., 1973, p. 148.

Captions of figures.

Figure 1. The trace, Γ, of a rigid cylinder in the physical plane and its image, C, in the hodograph plane.

Figure 2. A cylindrical, symmetrical airfoil is placed in a uniform flow with speed q_∞, so that the symmetry axis is parallel to the undisturbed fluid velocity.

Figure 3. The image of upper half of the airfoil contour in Fig. 2 is the curve C_A, and the image of the flow region above the symmetry axis of the airfoil is the region bounded by C_A and cut along the line section C_S on the u-axis from 0 to q_∞.

Figure 4. The fundamental solution in the subsonic region ($q < q_{crit}$) for $q' = 0$ shown as a function of u/q_{crit} and v/q_{crit}.

Figure 5. The fundamental solution in the subsonic region for $q' = 0.5 * q_{crit}$ and $\theta' = 0$.

Figure 6. Same as Fig. 5 except that $q' = 0.7 * q_{crit}$.

Figure 7. Same as Fig. 5 except that $q' = 0.8 * q_{crit}$.

Figure 8. Same as Fig. 5 except that $q' = 0.9 * q_{crit}$.

Figure 9. Same as Fig. 5 except that $q' = 0.95 * q_{crit}$.

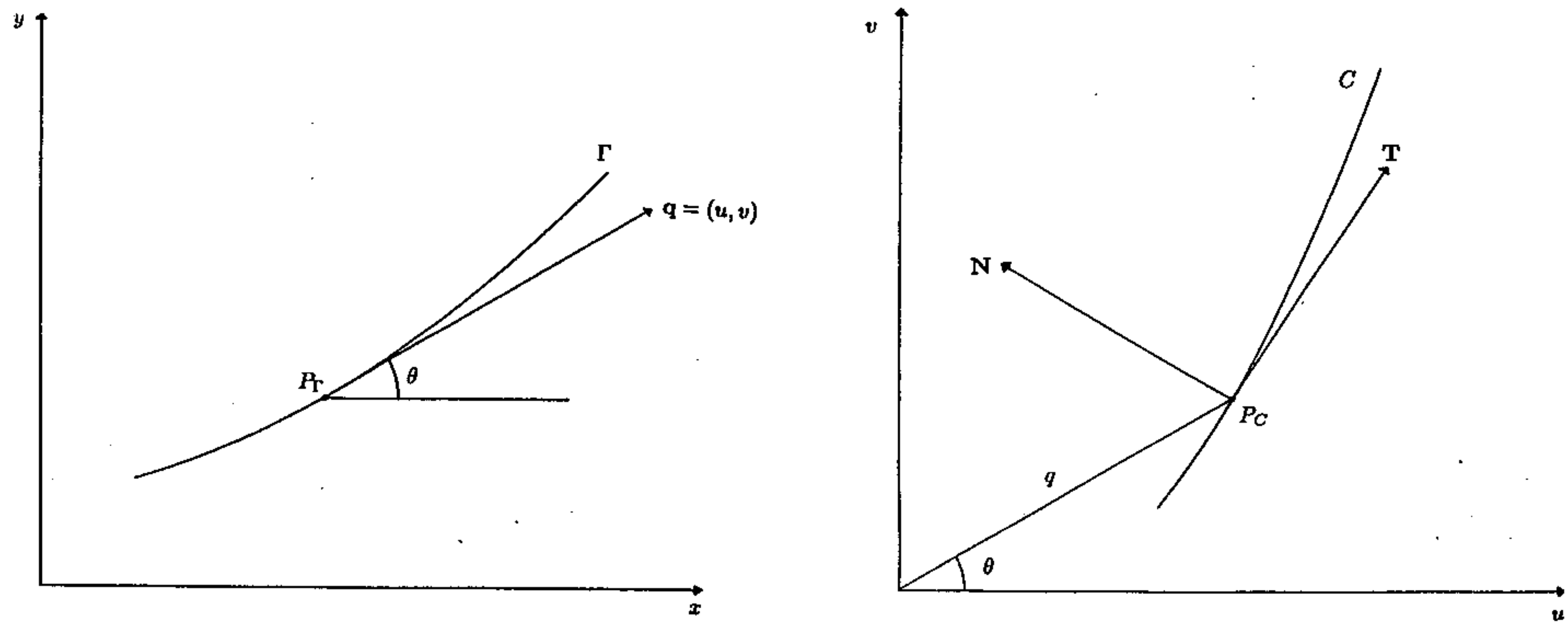

y
x
Γ
q = (u, v)
P_Γ
θ
v
u
C
T
N
P_C
q
θ

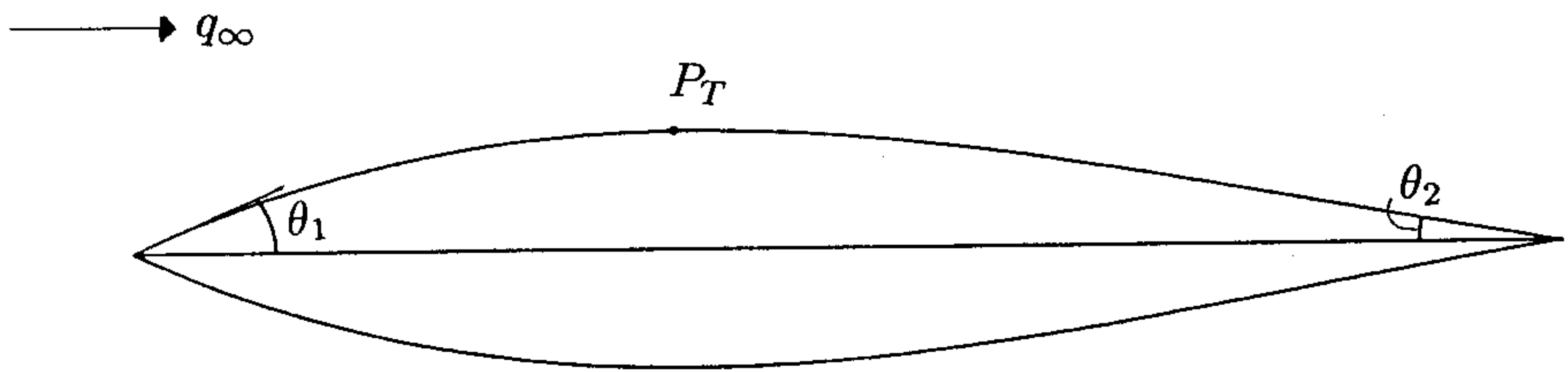

q_∞
P_T
θ_1
θ_2

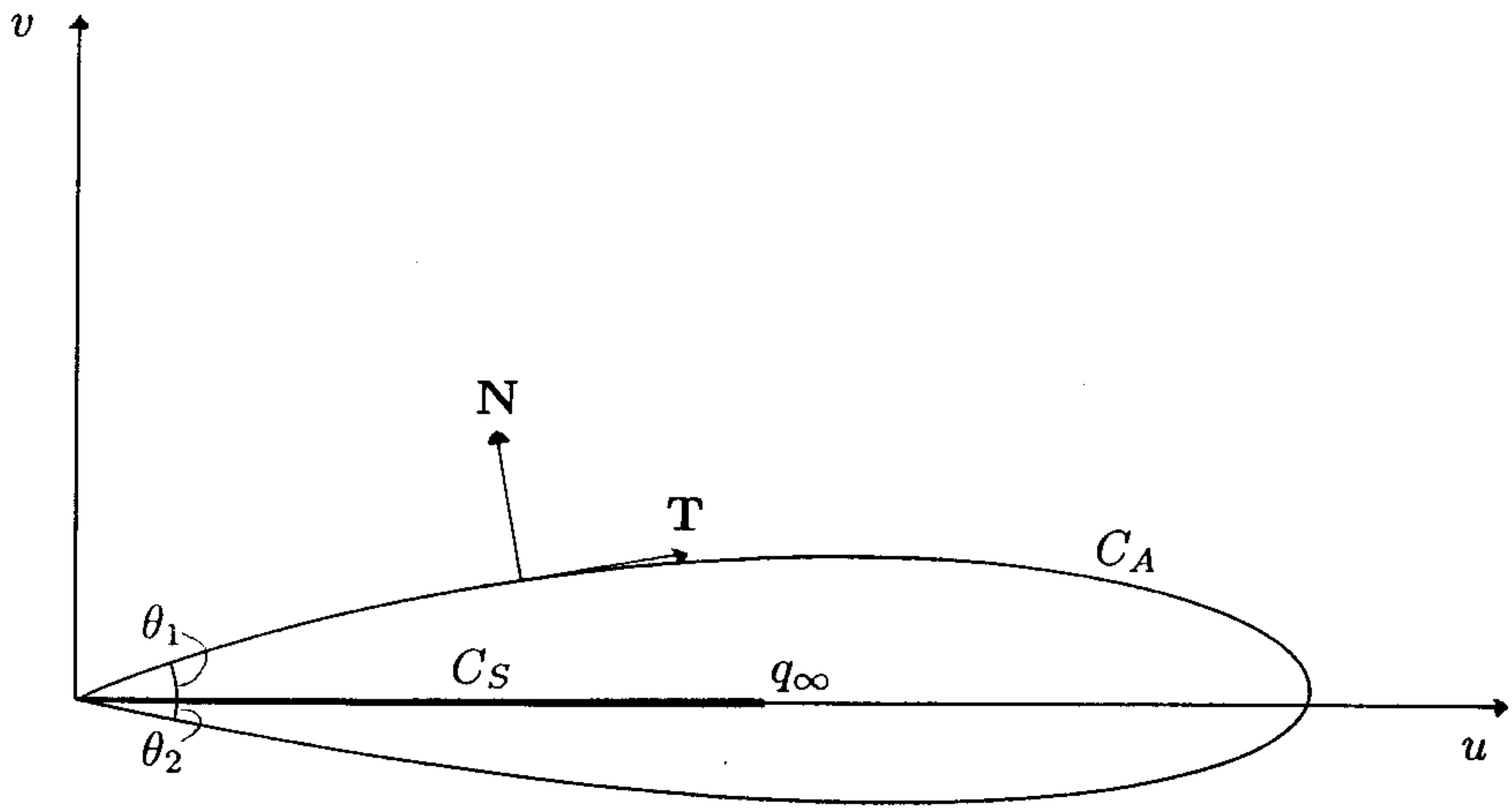

v
N
T
C_A
θ_1
C_S
q_∞
u
θ_2

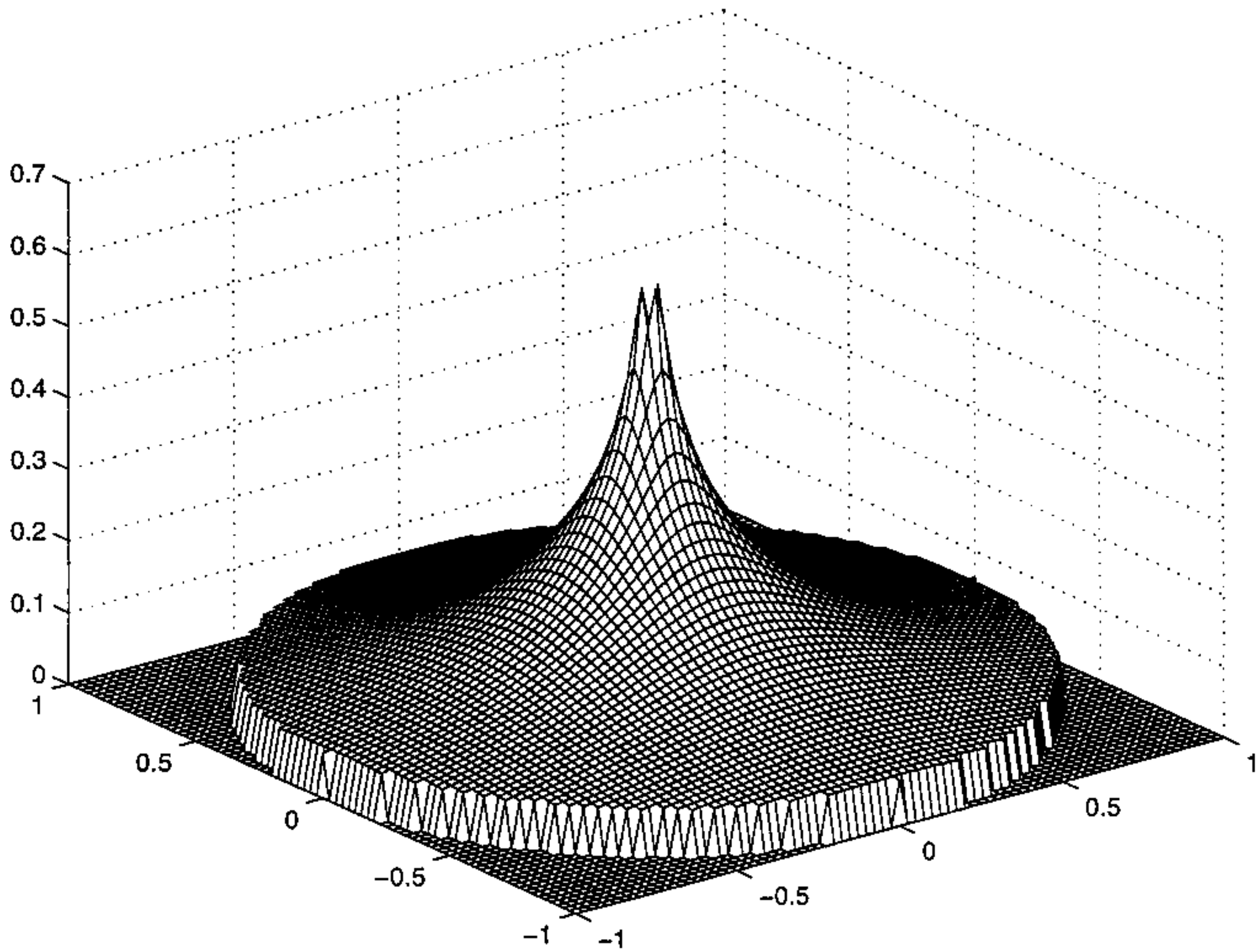
0.7
0.6
0.5
0.4
0.3
0.2
0.1
0
1
0.5
0
−0.5
−1
−1
−0.5
0
0.5
1

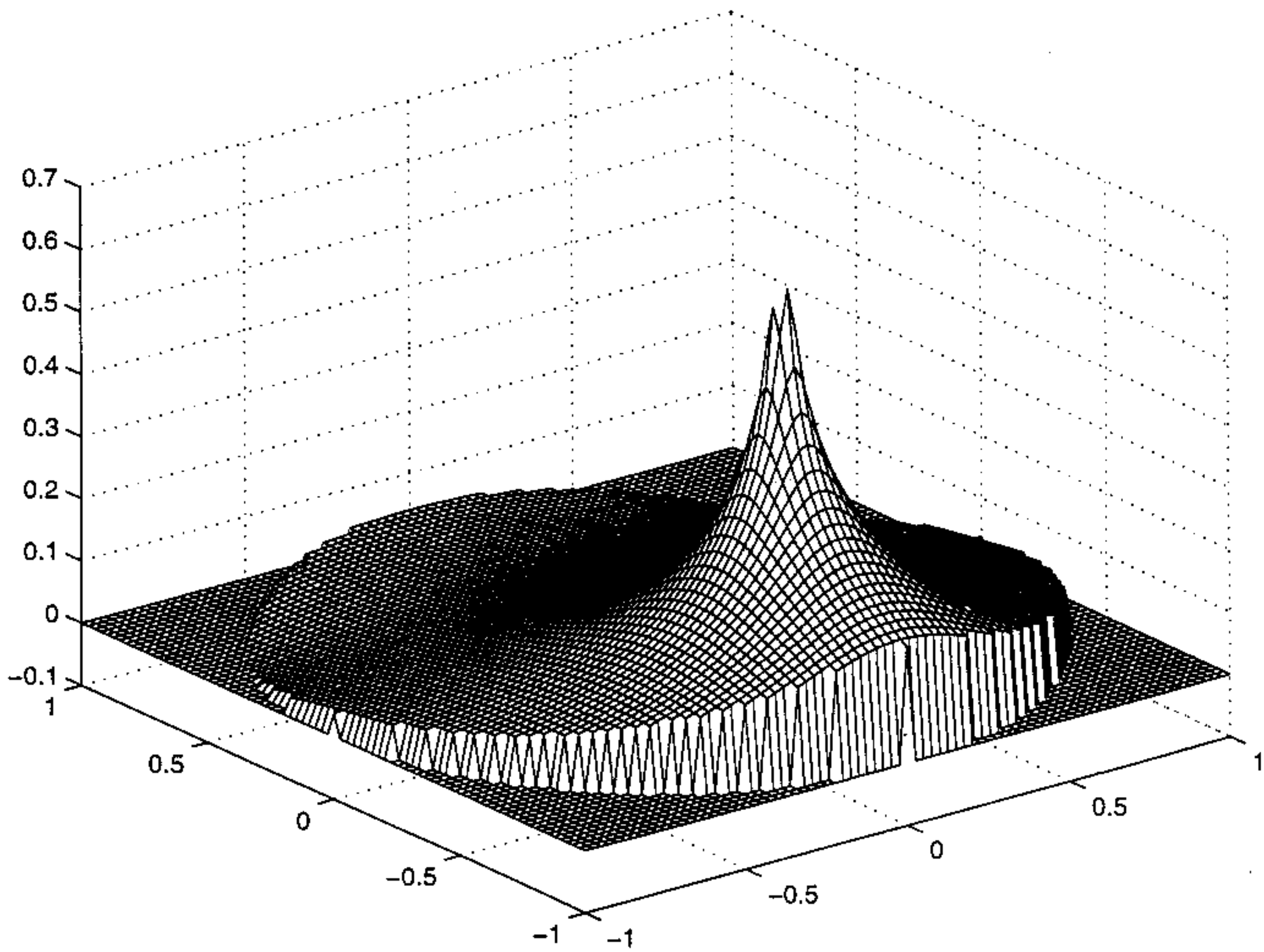

0.7
0.6
0.5
0.4
0.3
0.2
0.1
0
−0.1
1
0.5
0
−0.5
−1
−1
−0.5
0
0.5
1

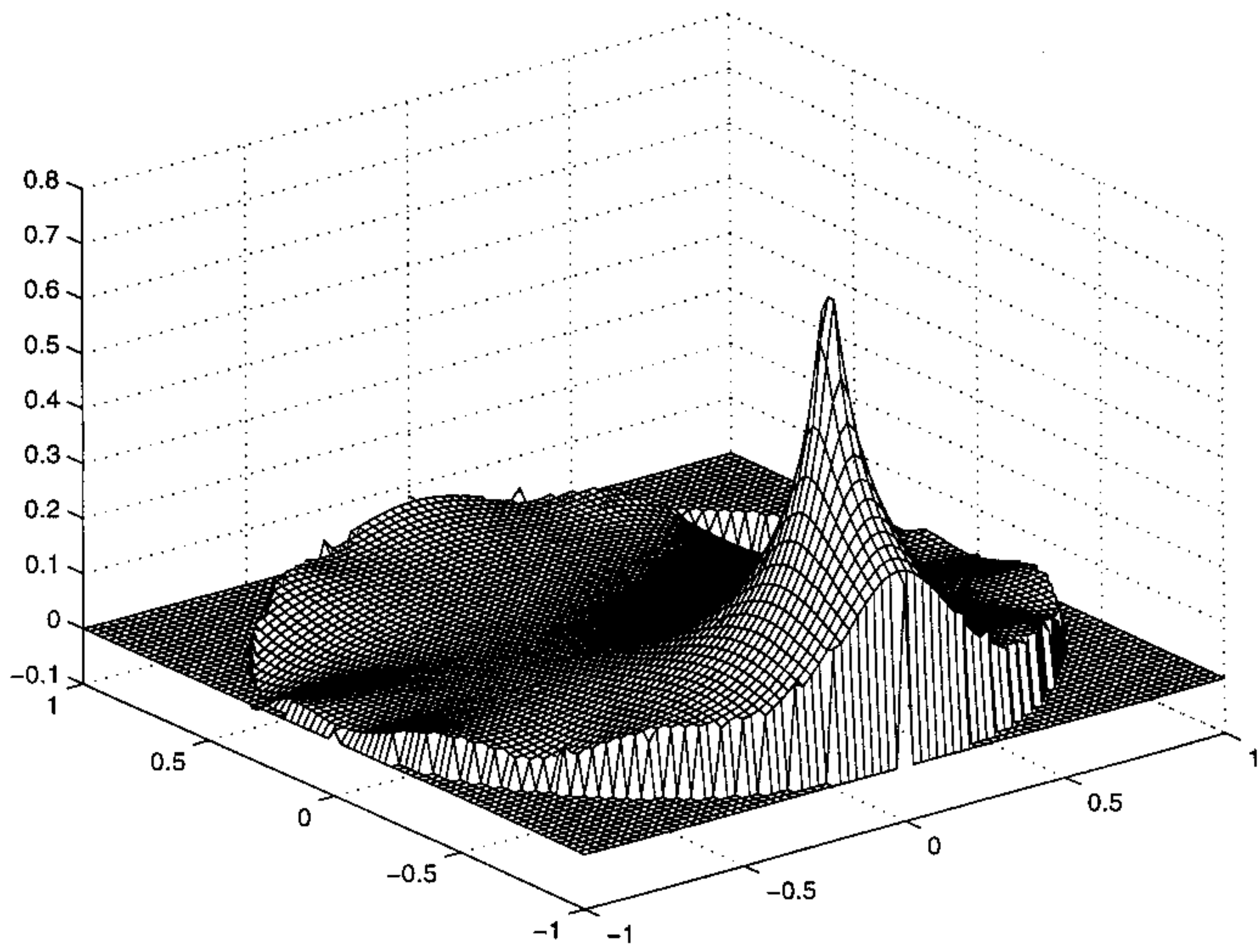

0.8
0.7
0.6
0.5
0.4
0.3
0.2
0.1
0
−0.1
1
0.5
0
−0.5
−1
−1
−0.5
0
0.5
1

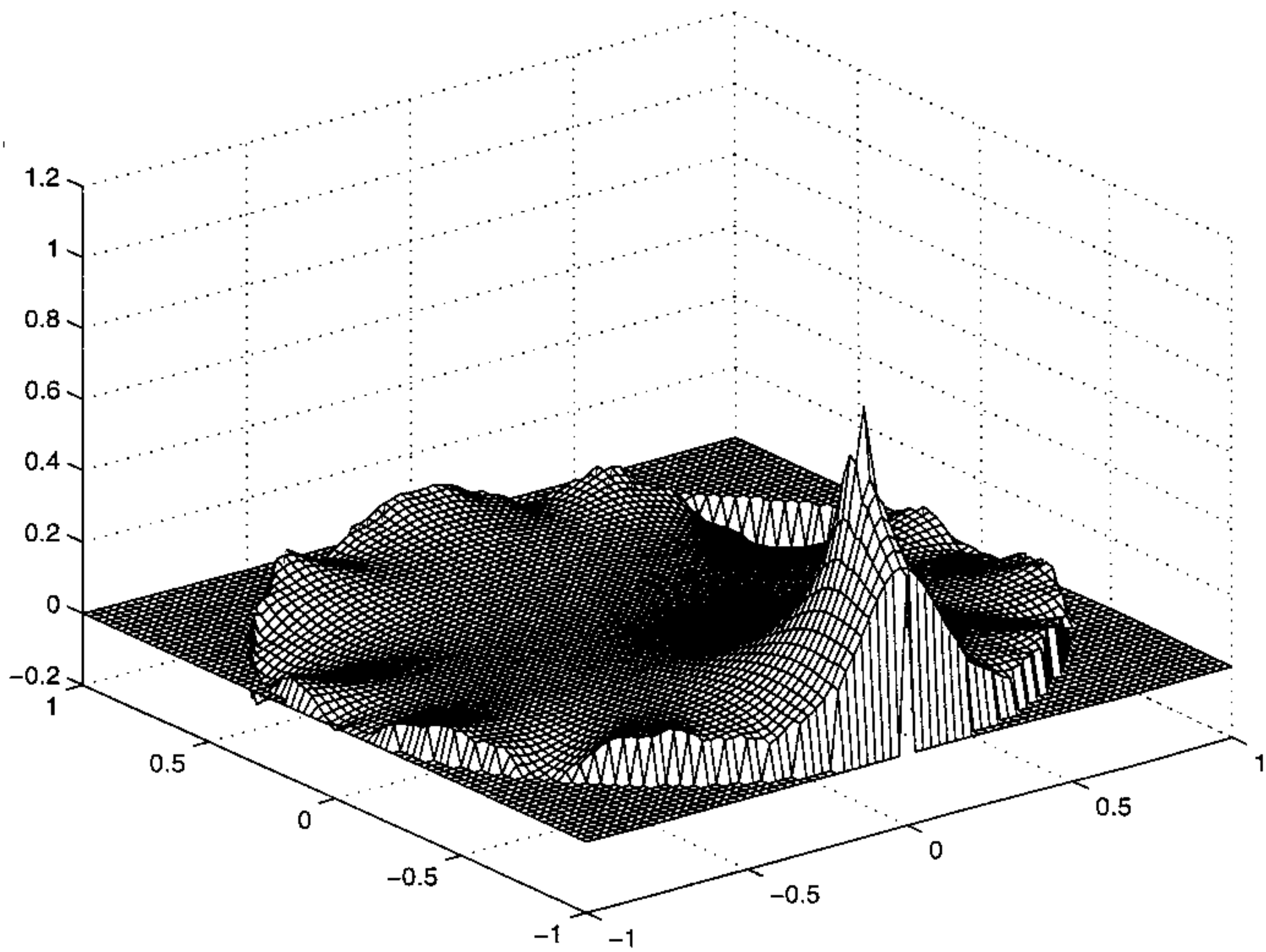

1.2
1
0.8
0.6
0.4
0.2
0
−0.2
1
0.5
0
−0.5
−1
−1
−0.5
0
0.5
1

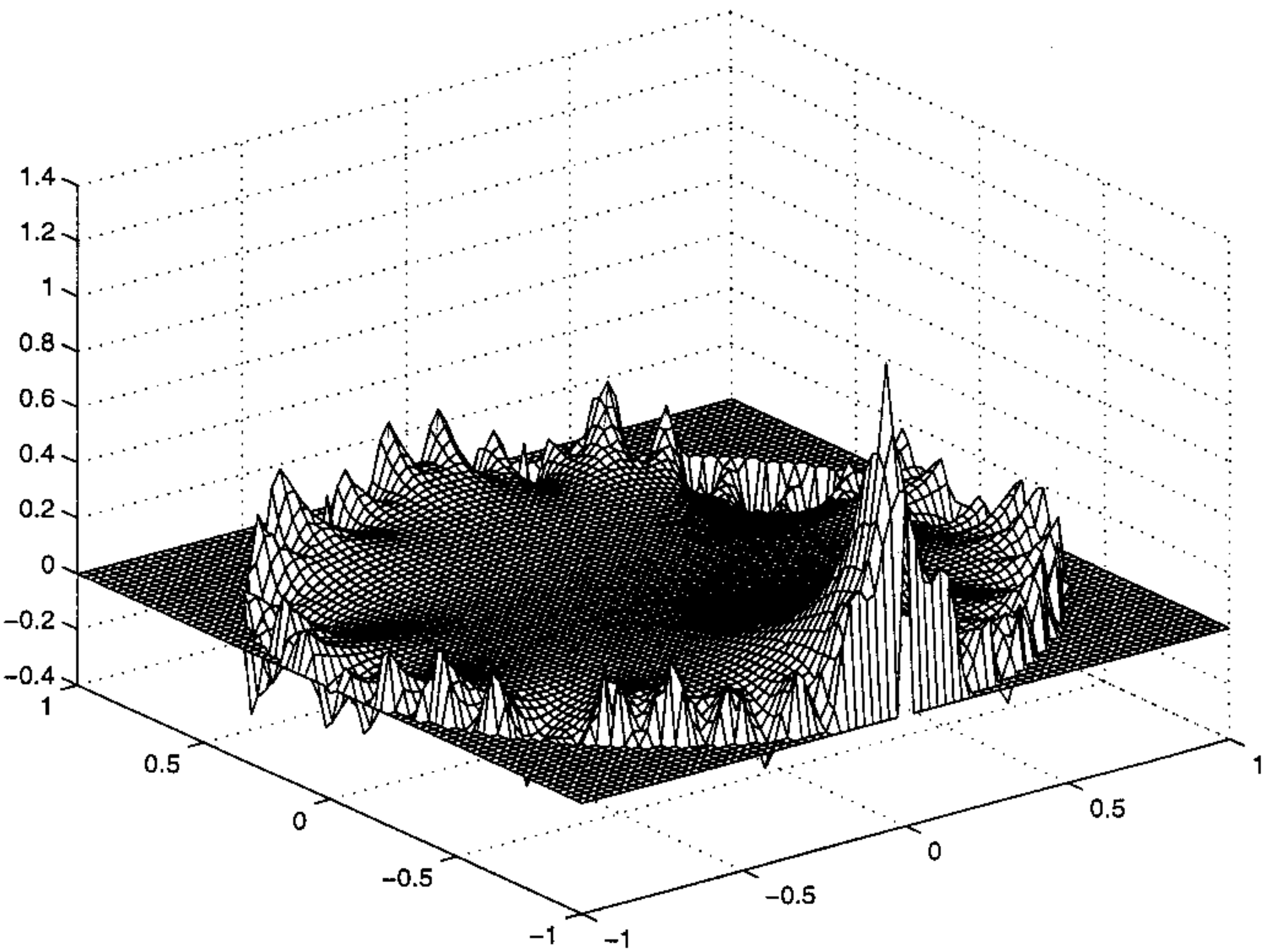
1.4
1.2
1
0.8
0.6
0.4
0.2
0
−0.2
−0.4
1
0.5
0
−0.5
−1
−1
−0.5
0
0.5
1

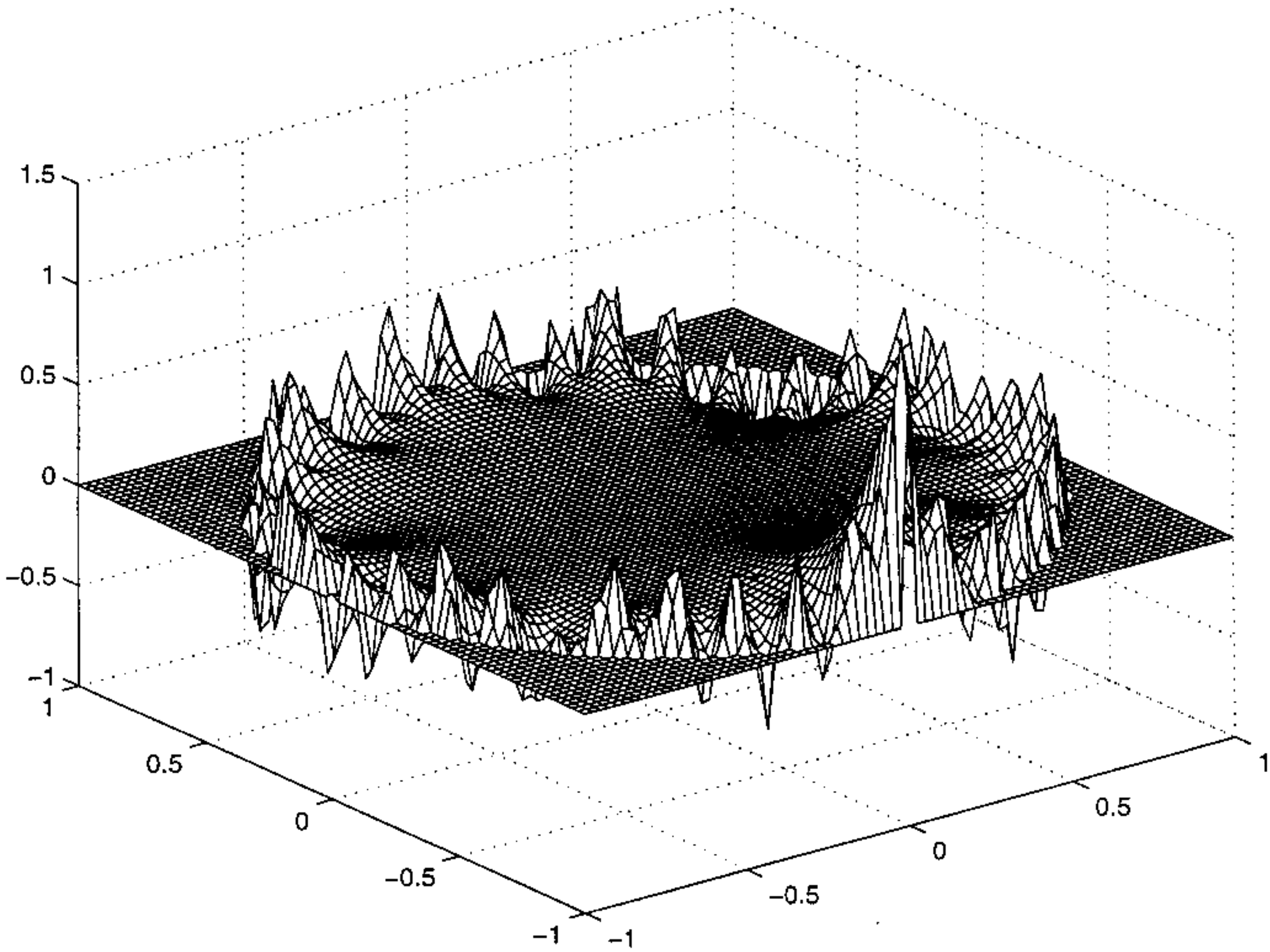
1.5
1
0.5
0
−0.5
−1
1
0.5
0
−0.5
−1
−1
−0.5
0
0.5
1